Efficient Radio Transmission with Adaptive and Distributed Beamforming for Intelligent WiMAX

Xiaohua Lian · Homayoun Nikookar · Leo P. Ligthart

Abstract   In this paper, we introduce Adaptive Beamforming (AB) and Distributed Beam-forming (DB) as two efficient techniques for Intelligent WiMAX (I-WiMAX). I-WiMAX is a new maritime communication system, consisting of Smart Radio (SR) principles and mobile WiMAX based on the IEEE 802.16e standard. Adopting AB, the same spectrum can accommodate more users by directing the main beam towards desired users while antenna pattern nulls towards others. To reduce the channel interferences caused by spectrum reusing, the Null Broadening (NB) method is required for downlink beamforming of I-WiMAX. A new NB method is presented in this paper with iterative weights computing for different OFDM subcarriers. Considering the spatial channel model seen at Subscriber Stations (SS) based on the von Mises distribution, the coverage range of one Base Station (BS) is dramatically enlarged by employing the NB technique. Meanwhile, assuming those SS which are within the coverage range as nodes of a relay network, the DB technique is introduced to forward signals to distant SS by forming the main beams towards them instead of deploying more BS to increase the communication range. It is proven in this paper that DB can successfully do the job. To reuse the spectrum, two DB methods are presented by directing different beams towards different required directions at the same time. With the AB and DB techniques, reliable I-WiMAX links can be established for long distances, with more optimum spectrum use and less infrastructure.

Keywords   Intelligent WiMAX · Smart radio · Adaptive beamforming · Distributed beamforming · Collaborative beamforming · Smart antenna · Adaptive OFDM

X. Lian (✉) · H. Nikookar · L. P. Ligthart
Department of Electrical Engineering, Mathematics and Computer Science, International Research Center for Telecommunications and Radar (IRCTR), Delft University of Technology, Mekelweg 4, 2628 CD Delft, The Netherlands
e-mail: x.lian@tudelft.nl

H. Nikookar
e-mail: h.nikookar@tudelft.nl

L. P. Ligthart
e-mail: l.p.ligthart@tudelft.nl

Abbreviations

AB	Adaptive Beamforming
AOFDM	Adaptive Orthogonal Frequency Division Multiplexed
AOA	Angle of Arrival
BS	Base Station
CDF	Cumulative Distributed Function
CMA	Constant Modulus Adaptive
DB	Distributed Beamforming
DOA	Direction of Arrival
DSS	Distant SS
FDD	Frequency Division Duplex
GPS	Global Positioning System
I-WiMAX	Intelligent WiMAX
LMS	Least Mean Square
MLM	Maximum Likelihood Method
MMSE	Minimum Mean Square Error
MS	Mobile Station
MVDR	Minimum Variance Distortion Response
NB	Null Broadening
NC	Null Constraint
OFDM	Orthogonal Frequency Division Multiplexed
Pdf	Probability density function
SA	Smart Antenna
SCORE	Spectrum self-COherent REstoral
SDMA	Space Division Multiple Access
SINR	Signal to Interference plus Noise Ratio
SIR	Signal to Interference Ratio
SMI	Sample Matrix Inversion
SNR	Signal to Noise Ratio
SR	Smart Radio
SS	Subscriber Station
TDD	Time Division Duplex
ULA	Uniform Linear Array
VDA	Virtual Direction Adding

1 Introduction

Beamforming techniques have been widely introduced to many wireless communication systems to improve the system Signal-to-Noise-Ratio (SNR), which will consequently increase system data rates and enlarge the coverage range. I-WiMAX has been introduced as a new maritime communication system which combines Smart Radio (SR) and Mobile WiMAX in an intelligent way [1]. This paper presents the applications of two different beamforming techniques to I-WiMAX: Adaptive Beamforming (AB) and Distributed Beamforming (DB).

1.1 I-WiMAX: A New Maritime Communication System

I-WiMAX is aimed to provide a metropolitan access network, and should offer higher bandwidth, larger coverage in maritime wireless communications compared to existing wireless
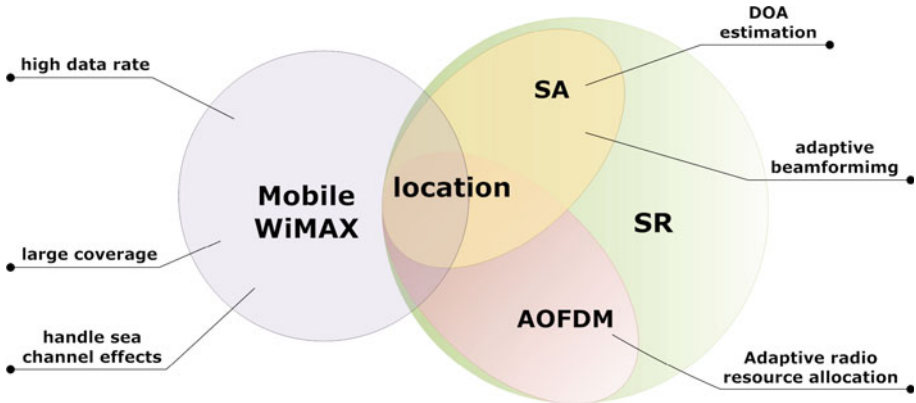
Fig. 1 I-WiMAX concept of maritime coastal/lake communications and locationing

systems. It is built upon SR and mobile WiMAX, as shown in Fig. 1 [1]. SR is a crucial part embedded in I-WiMAX to be applied into maritime communications. With SR, the new communication system gains knowledge on the severe sea communication environment, full of echoes and reflections, adapts to it, and therefore increases its cognition and flexibility. The SR technique, which is adopted on top of WiMAX, basically contains two techniques, Adaptive OFDM (AOFDM) and Smart Antenna (SA). AOFDM adaptively allocates the radio resource and consequently guarantees the reliable link in the sea channel full of fading and reflections caused by the rough sea surface. SA ensures a higher SNR which consequently results into larger coverage areas by performing adaptive beamforming.

With I-WiMAX, the people on board of ships are capable of enjoying a large amount of information anywhere and anytime. Therefore the transportation efficiency will be significantly improved by the abundant and versatile information obtained from the new maritime communication system based on broadband wireless networks. Furthermore the locationing ability of the broadband communication system is integrated, offering position services via RF localization.

1.2 Pervasive Adaptive Beamforming Techniques for Wireless Communications

SA is an effective technique for every energy-efficient radio because it can, in the transmit mode, focus the energy in the required direction and assist in reducing the multipath reflections and delay spread [2], caused by the fact that a desired signal can arrive via different directions [3]. In the receive mode, it can also perform optimal combining after delay compensation of the incoming multipath signals [4]. According to [5], an M-element adaptive array and a multi-beam antenna provide an M-fold increase in antenna gain. This increases the range and reduces the number of base stations required to cover a given area. An adaptive beamformer for the uplink WiMAX compliant system was proposed in [6], which has demonstrated its ability to cope with time varying interference effectively. For WiFi in maritime scenarios, it has been shown in [6] that if a sectorized antenna is employed instead of an omni-directional antenna, the distance tested in a boat-to-air experiment can be at least doubled.

Recently an experimental adaptive beamforming system for the IEEE802.16e-2005 OFDMA downlink has been implemented by Motorola labs [7,8]. This system consists
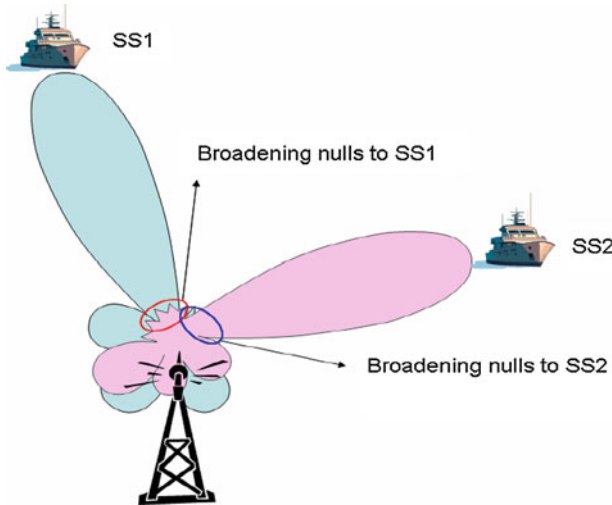
Fig. 2 Null broadening technique for an adaptive OFDM beamformer for I-WiMAX (SS1 and SS2 share the same OFDM subcarriers)

of a real time-division duplex link between the Base Station (BS) array antenna and a single antenna Subscriber Station (SS). The test results show that the Mobile WiMAX is capable of obtaining significant coherent processing gains allowed by array antenna channels. The requirements for supporting SA by WiMAX are discussed in detail in [9], as well as the protocol support and the complexity of extra signal processing as a result of beamforming.

In this paper, we propose an efficient spectrum usage of green radio, which means that all SS are assigned to all OFDM sub-carriers. Since we serve more than one user on a single traffic channel, co-channel interference suppression is our goal to achieve. Due to the spatial filtering function of SA, co-channel interferences may be reduced at both transmit and receive side by forming beams with nulls in the direction of those SS who share the same spectrum band [10–12]. As a result, it may lead to an increased number of users [13,14], which consequently improves the channel capacity and spectrum efficiency [15].

An uplink adaptive beamforming technique can direct its main beam towards the interested signal source, while displaying nulls to the unwanted directions. This ensures that the transmitted signal from one of the SS can be detected and selected by the BS via beamforming. Therefore, for those re-used OFDM sub-carriers, the weights should guarantee the main beam directed towards the desired SS, while at the same time "null" beams are created towards other SS.

For downlink, since SS does not have SA, appropriate beamforming techniques must be provided by the BS to satisfy the link quality for all co-channel SS. If we only use the estimated weights of uplink for the downlink, the nulls in the patterns towards those co-channel SS may become too narrow. Therefore, Null Broadening (NB) methods for beamforming should be considered [16]. Employing the NB technique, the adaptive downlink beamforming of I-WiMAX for green radio is shown in Fig. 2. Unlike the point nulling technique, the downlink beamforming with null broadening will spread the nulling over an angular region around a certain direction. I-WiMAX performs downlink beamforming with depressed power in a certain angular range to guarantee that the co-channel interference caused by spectrum reusing is reduced for SS.
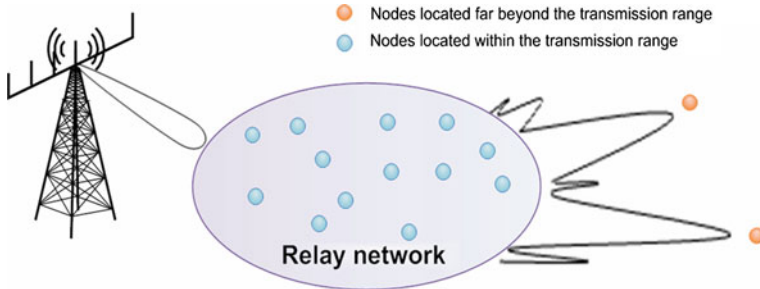
Fig. 3 Distributed beamforming for I-WiMAX in long distance communications

In this paper, we present a new NB method. It can be regarded simply as adding the coherent signals to each available signal source, but operating in two different directions; therefore it is called Virtual Direction Adding (VDA). Meanwhile, we also give a closed-form relationship between the weights of the Minimum Variance Distortionless Response (MVDR) beamformer and those with broadened nulls. Based on this result, we show that the weights of downlink beamforming with NB can be calculated iteratively. In addition, we demonstrate and compare VDA with another NB method, and show that when considering the spatial channel seen at the SS, the proposed NB method for downlink beamforming is highly required and it decreases co-channel interferences significantly.

1.3 Distributed Beamforming: A New Concept Beamforming Technique

In the case when some of the SS are beyond the transmitting range of each SS, we propose a solution to build a long distance energy-efficient link for I-WiMAX, as demonstrated in Fig. 3. We suggest the "close" SS, which are located within the transmission range, to form a relay network forwarding BS signals by employing a beamforming technique to "far" SS, which are beyond the transmission range. The BS is equipped with SA, and then it can steer the main beam towards the direction of the relay network. We assume that the main beam is wide enough, and then all the nodes share the same information simultaneously. All relay nodes will constructively display a spatial beam pattern, directing mains beams towards those "far" SS. With the energy focused only in these directions, signals can be transmitted properly to a distant SS. Consequently, the BS cell coverage can be enlarged significantly without needing extra infrastructure.

The difficulty of the beamforming shown in Fig. 3 is that the positions of SS in the relay network for I-WiMAX are random. Unlike fixed antenna array elements, each SS can appear anywhere within the coverage range. Therefore, another beamforming technique (which is based on distributed array antenna elements), rather than AB should be considered.

DB is originally employed as an energy-efficient scheme to solve the long distance transmission by wireless sensor networks, in order to reduce the amount of energy required and consequently to extend the utilization time of the sensors. The basic idea of DB is that a set of nodes in wireless networks are treated as a virtual antenna array and then form a beam towards a certain direction to collaboratively transmit a signal. The direction of the main beam can be adjusted by setting the initial phase of each node. It is also regarded as collaborative beamforming.

Based on the work in [17], DB is proposed in [18] as a new concept of beamforming. By employing N collaborative nodes, the collaborative beamforming can result in up to N-fold gain in the received power at a distance access point [18]. A cross-layer approach to DB for wireless ad-hoc networks is discussed in [19] with more complicated models and two time phases of communication steps. The improved beampattern and connectivity properties are shown in [20], and a reasonable beamforming performance with node synchronization error is discussed in [21]. DB requires accurate synchronization; in other words, the sources must transmit at the same time, synchronize their carrier frequencies and control their carrier phases so that their signals can be combined constructively at the destination. Several synchronization techniques for DB can be found in [22,23].

As shown in the model of Fig. 3, by introducing DB to the relay network, not only BS increases its transmission range, but also each SS as a collaborative relay node can reduce its transmission power to preserve its energy. As mentioned before, we propose that with the adaptive beamforming technique, the BS can transmit signals by steering the main beam towards one SS and nulls towards others while efficiently using the spectrum. This basic idea can also be implemented in DB for the relay network. It requires for the nodes of the relay network to form a beampattern with different main beams towards different directions of distant SS. If we adopt the initial phases proposed for each node as in [18], only a single main beam towards one direction can be generated at one time. Therefore, we need to separately form different main beams in divided time slots, which is not time-efficient. Meanwhile, synchronizing the initial phases of nodes in each sub-time slots will also be required.

In this paper, we present two DB methods that can form multi-beams. The first method is to separate the nodes geographically into several ring ranges and a smaller circular range, while nodes at different ranges adopt different initial phases. Then by combining them together constructively, we can have beams towards several required directions. Another technique is to assign initial phases to each node randomly. Both DB methods can display multi-beam towards different destinations successfully, and only require one time of synchronization, instead of nodes synchronized each time when the beam direction changes. The Cumulative Distributed Function (CDF) of the beampattern, when the number of nodes is large, is discussed, showing the probability of a certain amount of energy that can be received at different directions.

1.4 Organization of the Paper

This paper is organized as follows. First in Sect. 2, we discuss AB for I-WiMAX. This includes the uplink and downlink Adaptive Beamformers. Meanwhile, a new NB method as a co-channel interference reduction technique is shown and demonstrated. In Sect. 3, DB for I-WiMAX is explained. We show that with two multi-beam generating DB methods, I-WiMAX is able to achieve communications to SS which are far beyond the transmission range. Finally in Sect. 4, we conclude the paper.

2 Adaptive Beamforming Technique for I-WiMAX

In this section we demonstrate that the adaptive beamformers for I-WiMAX allow for efficient spectrum re-using. Both uplink and downlink adaptive beamformers are discussed. Particularly, a new NB method is presented.
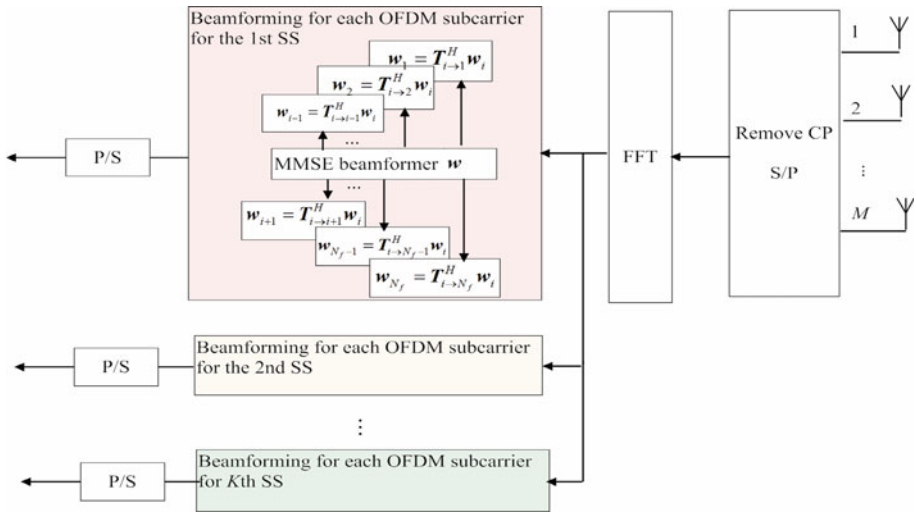
Fig. 4 Adaptive uplink OFDM beamformer of I-WiMAX (P/S: Parallel to Serial; FFT: Fast Fourier Transform; CP: Cyclic Prefix; S/P: Serial to Parallel; N_f: number of OFDM subcarriers)

2.1 Uplink and Downlink Adaptive Beamforming for I-WiMAX

The uplink adaptive OFDM beamformer of I-WiMAX is illustrated in Fig. 4. The Minimum Mean Square Error (MMSE) beamformer is situated after the FFT for receiving. This is why it is called the post-IFFT/FFT beamformer. Its basic idea is to regard OFDM signals as a combination of several narrowband signals, so that the weights of the MMSE beamformer are decided after the Multi-carrier Modulator/Demodulator (IFFT/FFT) for each OFDM subcarrier. The weights for the OFDM adaptive beamformer are calculated iteratively. As shown in Fig. 4, if one set of weight $\mathbf{w}_i$ for the ith OFDM subcarrier is computed, others will be deduced by mapping them into different frequency bands via transformation matrix $\boldsymbol{T}$. Thus the beamforming calculation will be performed only K times for all K SS, which requires less computation load and consumes less time [24].

Several beamforming approaches exist with a varying degree of complexity. The beamforming technique was initially developed in the 1960s for military applications in sonar and radar, in order to remove unwanted noise and jamming from the array output. The first fully adaptive array was conceived in 1965 by Applebaum in [25,26], which was designed to maximize the SNR at the array's output. The Least Mean Square (LMS) error algorithm proposed by Widrow in [27] was regarded as an alternative approach to cancelling the unwanted interferences. Further work about LMS techniques was done by Frost in [28] and Griffiths in [29] by introducing the constraints to ensure that the desired signals were not filtered out along with the unwanted signals. However, for stationary signals, both algorithms converge to the optimum Wiener solution [30]. A different technology presented by Capon in 1969 [31] was the mentioned MVDR or the Maximum Likelihood Method (MLM). This was the first attempt to automatically localize signal sources. Later in 1974, the Sample Matrix Inversion (SMI) technique, which determines the adaptive antenna array weights directly, was demonstrated in [32]. These all belong to time-dependent reference techniques, which optimize the receive antenna weights in order to identify a known sequence at the output of the antenna array. Another technique is called the spatial reference technique, based on the

Direction Of Arrival (DOA) estimation of signal sources. Many estimation methods of wave number and DOA of signal sources can be found in [33–35]. Blind beamforming is another important beamforming technique, which does not require training sequences and any information concerning the array's geometries: for example, Constant Modulus Adaptive (CMA) beamforming in [36], Constant Modulus (CM) in [37], Spectrum self-COherent REstoral (SCORE) in [29–39] and Decision-Directed Algorithm (DDA) beamforming in [40,41]. To improve the robustness to the DOA uncertainty, the Bayesian beamformer was also proposed in [42,43].

For beamforming in the downlink, the weights for each subcarrier can also be calculated iteratively. Several methods [44–46] have been presented to derive the weights for downlink based on the knowledge of those of uplink, for example, the Null Constraint (NC) weights deciding approach.

2.2 A New NB Beamforming Technique for Downlink

We propose a new NB method, called VDA, on top of the MVDR beamformer employed for downlink beamforming by the I-WiMAX BS.

NB technique was originally developed as a robust array beamforming technique. It was also regarded as a beampattern synthesis method. Mailoux in [47] presented a NB method by a simple modification of the covariance matrix of the received signal. While in [48], a similar NB algorithm was also presented by applying a transform to the same covariance matrix. Both methods were capable of providing a notch at the locations of interferences signals. In [49], two NB algorithms as Covariance Matrix Taper (CMT) methods are defined, and considered as effective robust adaptive beamforming techniques, imparting robustness into the adaptive pattern by a judicious choice of null placement and width. In [50,51], it was proved that NB was able to extract moving targets with less number of snapshots for the covariance matrix in sonar applications. As for wireless communication, NB was employed in a cellular communication system [52], and particularly an example was given in Space Division Multiple Access (SDMA) system for downlink beamforming [53]. In [53], three different NB schemes were compared. They were the Angular Spread (AS) based approach, high order NB and multiple nulling. All of them were shown to increase the Signal to Interference plus Noise Ratio (SINR) at the Mobile Station (MS). What is more, it also illustrated that NB for downlink beamforming was quite essential in the propagation environment with AS. Recently in [54], a constrained optimization approach for NB has been proposed, which was based on semi-definite programming. This NB method could also broaden the main beam for desired detection and consequently it achieved a better coverage. Another iterative NB method was discussed in [55] for depressing side lobes in applications of array beampattern synthesis with lower number of interference signals and high iteration speed.

We assume that the BS is equipped with a Uniform Linear Array (ULA) containing M antenna elements. There are K far-field SS. We first discuss VDA based on narrowband signal sources, and then we show how to calculate iteratively the whole set of weights with NB of OFDM signals.

The received signal of the BS is given by:

$$\mathbf{x}(t) = \sum_{i=1}^{K} \mathbf{a}(\theta_i)s_i(t) + \mathbf{n}(t), \quad t = 1, 2, \ldots, L \tag{1}$$

where L is the number of snapshots, $\mathbf{a}(\theta_i)$ is the steering vector of the ith signal sources in the direction of θ_i,

$$\mathbf{a}(\theta_i) = \left(1, e^{-j\frac{2\pi}{\lambda}d\sin(\theta_i)}, \ldots, e^{-j(M-1)\frac{2\pi}{\lambda}d\sin(\theta_i)}\right)^T, \quad i = 1, 2, \ldots, K \tag{2}$$

T is the vector transpose. $s_i(t), i = 1, 2, \ldots, K$ are the signals from all SS and $\boldsymbol{n}(t)$ is the Additive White Gaussian Noise (AWGN). Parameter d is the space between two array elements, and λ is the wavelength.

The received covariance matrix at the BS equals:

$$\boldsymbol{R}_{\text{uplink}} = \text{E}[\boldsymbol{x}\boldsymbol{x}^H] = \sum_{i=1}^{K} \sigma_i^2 \boldsymbol{a}(\theta_i)\boldsymbol{a}^H(\theta_i) + \sigma_n^2 \boldsymbol{I} \tag{3}$$

where superscript H means hermitian transpose, and $\sigma_i^2, i = 1, 2, \ldots, K$ is the power of the ith signal and σ_n^2 is the variance of the noise.

We then can estimate $\boldsymbol{a}(\theta_i), \sigma_i^2, \sigma_n^2$ by $\widehat{\boldsymbol{a}}(\theta_i), i = 1, 2, \ldots, K, \widehat{\sigma}_i^2, i = 1, 2, \ldots, K$ and $\widehat{\sigma}_n^2$, which help us to calculate the covariance matrix for the downlink beamformer of the kth user,

$$\boldsymbol{R}_k = \sum_{i=1, i \neq k}^{K} \widehat{\sigma}_i^2 \widehat{\boldsymbol{a}}(\theta_i)\widehat{\boldsymbol{a}}^H(\theta_i) + \widehat{\sigma}_n^2 \boldsymbol{I} \tag{4}$$

The well-known CMT method is fully employed for the uplink mode. However, when it is introduced for downlink beamforming, it needs to reconstruct the covariance matrix for the kth SS at downlink by estimating the DOA and powers of SS and also of the noise power, as shown in (4).

The weights of MVDR beamformer are [56]:

$$\boldsymbol{w}_k = \boldsymbol{R}_k^{-1}\widehat{\boldsymbol{a}}(\theta_k)/(\widehat{\boldsymbol{a}}^H(\theta_k)\boldsymbol{R}_k^{-1}\widehat{\boldsymbol{a}}(\theta_k)) \tag{5}$$

In order to produce a notch of width W in each interference direction, the CMT method is required to calculate $\widetilde{\boldsymbol{R}}_{\text{CMT},k}$ by the Hadamard product of $\boldsymbol{R}_k$ and $\boldsymbol{T}$:

$$\widetilde{\boldsymbol{R}}_{\text{CMT},k} = \boldsymbol{R}_k^{\circ}\boldsymbol{T} \tag{6}$$

where

$$(\boldsymbol{T})_{m,n} = \text{sinc}[(m-n)W/2] \tag{7}$$

represents the element of matrix $\boldsymbol{T}$, located at the mth row and the nth column. Then by using $\widetilde{\boldsymbol{R}}_{\text{CMT},k}$ in (5) instead of $\boldsymbol{R}_k$, we can have the weights with NB calculated by CMT.

By using an approximation for the sinc function,

$$\text{sinc}(x) \approx 1 - \frac{4}{3}sin^2\left(\frac{\pi x}{3}\right), \quad x \ll 1 \tag{8}$$

The null broadening $\widetilde{\boldsymbol{R}}_k$ in the new NB method is calculated from:

$$\widetilde{\boldsymbol{R}}_k = \frac{1}{3}\boldsymbol{R}_k + \frac{2}{3}\boldsymbol{D}_1\boldsymbol{R}_k\boldsymbol{D}_1 + \frac{2}{3}\boldsymbol{D}_2\boldsymbol{R}_k\boldsymbol{D}_2 \tag{9}$$

where

$$\boldsymbol{D}_1 = \text{diag}\left(\left[1, \cos\left(\frac{\pi W}{3}\right), \ldots, \cos\left(\frac{\pi W(M-1)}{3}\right)\right]^T\right) \tag{10}$$

$$\boldsymbol{D}_2 = \text{diag}\left(\left[1, \sin\left(\frac{\pi W}{3}\right), \ldots, \sin\left(\frac{\pi W(M-1)}{3}\right)\right]^T\right) \tag{11}$$

diag($\boldsymbol{\beta}$) spans a diagonal matrix with each element of vector $\boldsymbol{\beta}$ on the main diagonal.
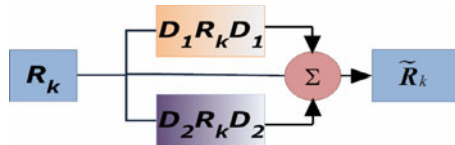
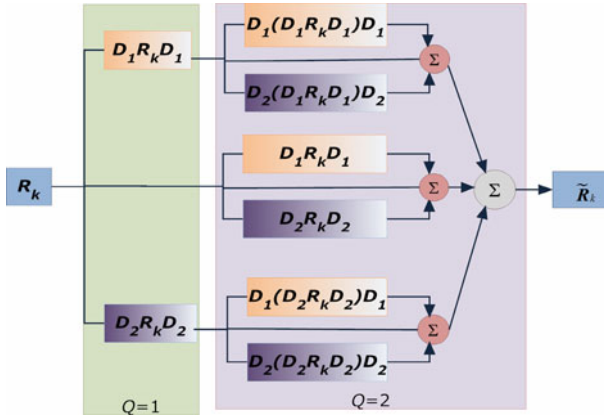**Fig. 5** Reconstructed covariance matrix for NB

Fig. 6 The two-step iterative VDA

The proof of equation (9) is shown in Appendix A.

Similarly, if we adopt $\widetilde{R}_k$ instead of R_k in (5), we can compute the weights $\widetilde{w}_k$ of VDA. VDA can be performed by adding two directions with coherent signal sources to the received signals. Expressions (4) and (9) illustrate that the modification of the received signal at downlink of the kth SS consists of 3 parts. The first is the received signal $x(t)$ but without $a(\theta_k)s_k(t)$, i.e., eliminating the signal from the kth SS. The other two parts are considered as the coherent signals coming from directions $\cos\left(\frac{\pi W}{3}\right) e^{j\frac{2\pi}{\lambda}\sin(\theta_i)}$ and $\sin\left(\frac{\pi W}{3}\right) e^{j\frac{2\pi}{\lambda}\sin(\theta_i)}$ with $i \neq k, i = 1, 2, \ldots, K$. The reconstructed covariance matrix of $\widetilde{R}_k$ is shown in Fig. 5.

In order to put deeper nulls around the required directions, the VDA can be calculated iteratively. A two-step iterative method is demonstrated in Fig. 6. To keep the same width, the starting width W_0 is chosen as

$$W_0 = \frac{W}{2^Q - 1} \tag{12}$$

where Q is the total number of iterations.

If the weights for the downlink MVDR beamformer are calculated as w_k in Eq. (5), we derive

$$\widetilde{w}_k = (\widetilde{R}_k C^{-1} + I)^{-1} w_k \tag{13}$$

where

$$C = 2D_1 \widetilde{R}_k D_1 + 2D_2 \widetilde{R}_k D_2 \tag{14}$$

It is worth noticing that the weights of the MVDR and MMSE beamformer are both given by the Wiener solution. As a result, w_k of MVDR can also be calculated iteratively as w_k of the MMSE, which was shown in Fig. 4. For the NB case, if we let $U_k \overset{\Delta}{=} (\widetilde{R}_k C^{-1} + I)^{-1}$, the different weights of different subcarriers can then be computed iteratively by:
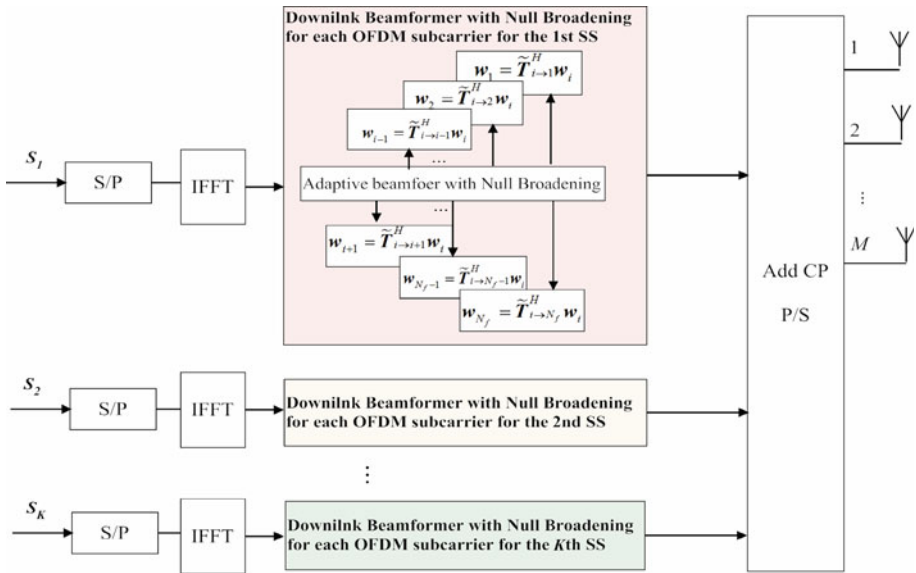
Fig. 7 Adaptive downlink OFDM beamformer with Null Broadening of I-WiMAX (S/P: Serial to Parallel; IFFT: Inverse Fast Fourier Transform; CP: Cyclic Prefix; P/S: Parallel to Serial; N_f: number of OFDM subcarriers)

$$\widetilde{w}_{k,i+1} = U_k T_{i \to i+1} w_{k,i} = U_k T_{i \to i+1} U_k^{-1} \widetilde{w}_{k,i} = \widetilde{T}_{i \to i+1} \widetilde{w}_{k,i} \tag{15}$$

The adaptive downlink OFDM beamformer with NB is shown in Fig. 7. The weights of each subcarriers for kth SS are deduced iteratively by multiplying the weights with $\widetilde{T}_{i \to i+1}$, where $\widetilde{T}_{i \to i+1} \stackrel{\Delta}{=} U_k T_{i \to i+1} U_k^{-1}$.

2.3 Simulation Results and Radio Spectrum Efficiency Improvement

A ULA with 16 elements at half-wavelength spacing is here taken into account ($M = 16$, $d = \lambda/2$). We assume that there are four SS, the four DOA's are at $\theta_1 = -17.5°, \theta_2 = -36.9°, \theta_3 = 23.6°, \theta_4 = 0$ ($\sin\theta_1 = -0.3, \sin\theta_2 = -0.6, \sin\theta_3 = 0.4, \sin\theta_4 = 0$) respectively. The SNR of the four SS are all 15dB. Since OFDM signals per subcarrier can be considered as narrow band, we only consider the narrow band case for simplicity. However, as can been seen in Fig. 7, the weights of VDA can be computed iteratively, meaning that the weights of different OFDM subcarriers are also easily calculated. We assume that all the SS are sharing the same spectrum band. As mentioned before, the adaptive beamformer assures for SS1 that the weights of each subcarrier should have nulls towards other three SS. The width of the notch is set to $W = 0.2$. We consider $Q = 2$ steps for iteratively using VDA. All the simulations are under the condition that $L = 500$.

Figure 8 shows the beampattern of the two methods, i.e., CMT and VDA. Figure 8 learns that both methods can broaden nulls towards the three directions of SS2, SS3 and SS4 with the same width $W = 0.2$, while directing the main beam to SS1. However, VDA can put deeper nulls to the angular around direction of SS2, SS3 and SS4 than CMT.

Figure 9 shows the CDF of the downlink power in the requested null broadening angles for SS2. We performed simulations for 5,000 times. It shows that CMT and VDA can depress
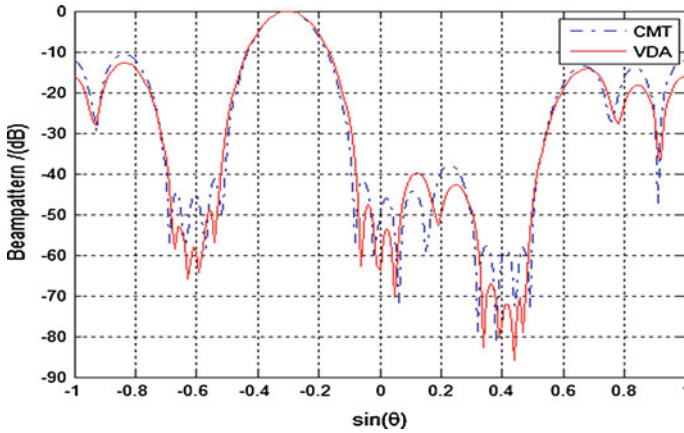
Fig. 8 Beampattern of two NB methods: CMT and VDA with for SS
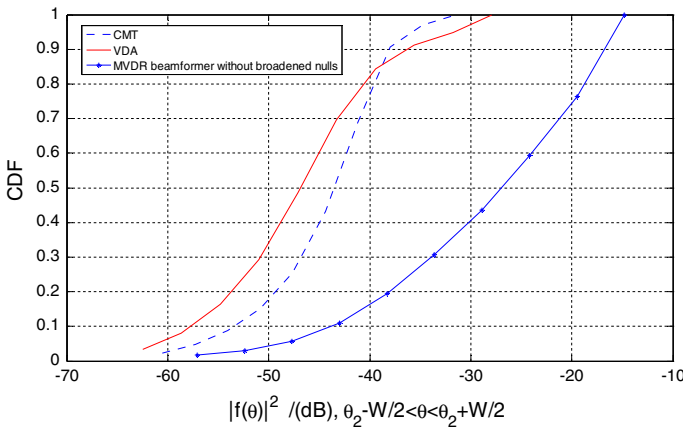

Fig. 9 CDF of the co-channel interferences depression for SS2

the power around the directions of SS2 by more than -30 dB. Figure 9 also illustrates that for 50% of time, VDA places the nulls with depth lower than -47 dB, while the CMT show deeper nulls than -47 dB for only about 30%. The worst performance of depressing interference at SS2 is given by adopting the MVDR beamformer without broadened nulls, which shows that there is only 8% of time that SS2 has a depression of co channel interference lower than -47 dB.

Next, we take the channel effect into the consideration. The received signal and power spectra at the SS depend on the probability density function (pdf) of the Angle of Arrival (AOA) of the scattered wave. Clarke considered a uniform AOA pdf over $[-\pi, \pi)$ [57]. However, it has been argued and experimentally demonstrated that the scattering encountered in many environments results into a non-uniform pdf of AOA at SS [58]. Reference [59] suggests the two-parameter Von Mises pdf as a flexible and generalized model for the pdf of AOA, which includes non-istropic scattering cases, and also the isotropic one as a special case. The pdf is given as [59],
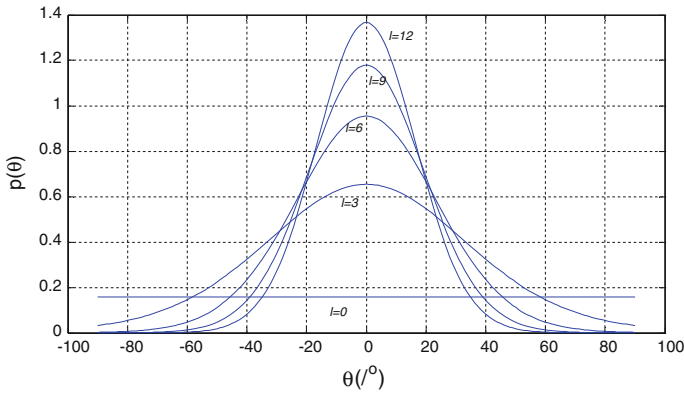
Fig. 10 Von Mises pdf for the AOA of scatter components at SS with different l, $\theta_p = 0$

$$p_\Theta(\theta) = \frac{\exp(l\cos(\theta - \theta_p))}{2\pi I_0(l)}, \quad \theta \in [-\pi, \pi) \tag{16}$$

where $I_0(k)$ is the zero-order modified Bessel function, θ_p accounts for the main direction of the AOA scatter components. Parameter $l \geq 0$ controls the width of the AOA of scatter components. Figure 10 shows the $p_\Theta(\theta)$ with different l for $\theta_p = 0$.

Based on Von Mises model, point nulls which can be generated by adaptive beamformers are not sufficient enough for energy depression, because the power around the nulling direction may also leak into other SS due to spatial scattering.

Assuming that there are K SS. The kth SS receives signals of powers $\{E_1, E_2, \ldots, E_K\}$ from all K users. The downlink Signal to Interference Ratio (SIR) for the kth user is defined as [55],

$$\eta_k = \frac{E_k}{\sum_{i=1, i\neq k}^{K} E_i} \tag{17}$$

With η_k, the coverage performance can be represented by the probability distribution function $C(\gamma) = P\{\eta_k > \gamma\}$. In our case, $K = 4$. Figures 11 and 12 compare the coverage performance of the three beamforming methods with different l connected to the Von Mises pdf. It can be seen that both VDA and CMT have a higher CDF than the MVDR beamformer without NB. As a result, the coverage range is significantly enlarged by the NB methods. According to Fig. 11, the chances of VDA and CMT methods to have a SIR of SS2 lower than -18 dB reaches 100 and 55% respectively, while that of MVDR without NB is less 10% with $l = 10$. When $l = 7$, the CDF in total is lower than that of $l = 10$; this is because the AOA pdf of the channel seen at SS is wider than that for $l = 10$, as indicated in Fig. 10. However, the VDA still achieves the best among the three.

3 Distributed Beamforming for I-WiMAX

In this section, we introduce DB to I-WiMAX for long distance communications beyond the coverage range of one BS. As shown in Fig. 3, accessible SS are regarded as wireless relays, and consequently they form a relay network with flexible and uncertain locations of each node. We first show the feasibility of DB for I-WIMAX. Then we present a new DB method
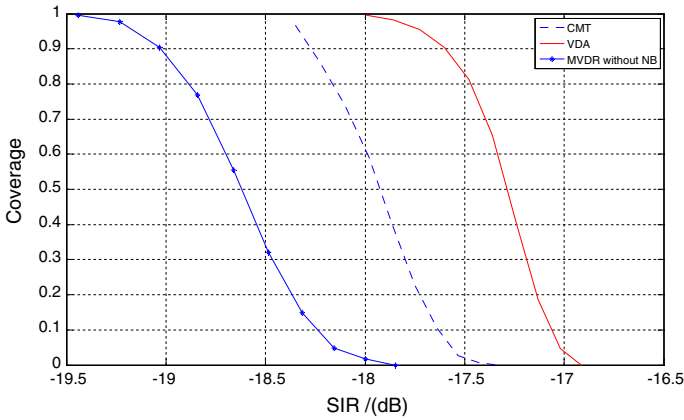
Fig. 11 Coverage performance of CMT, VDA and MVDR beamformer without NB when $l = 10$
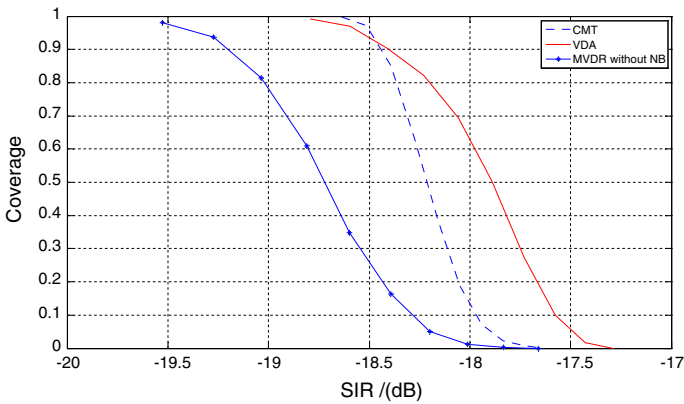

Fig. 12 Coverage performance of CMT, VDA and MVDR beamformer without NB when $l = 7$

to generate different beams towards different users at the same time, rather than in different time slots. Later we show some simulation results of the method based on OFDM signals.

3.1 DB for I-WiMAX in TDD and FDD Schemes

WiMAX supports two duplexing schemes: Time Division Duplex (TDD) and Frequency Division Duplex (FDD). However, most WiMAX implementations will likely use TDD, because it allows the system operator to receive the most from their investment in spectrum and telecom equipment, while meeting the needs of each individual user. We demonstrate here that TDD is also more suitable for the application of DB to I-WiMAX than FDD.

Figures 13 and 14 show DB for I-WiMAX in both TDD and FDD schemes. We mark those SS, which are beyond the transmission range as Distant SS (DSS). The uplink defines the link from DSS to BS, while downlink represents the reverse. In TDD mode, as shown in Fig. 13, DSS, SS and BS require only one channel for uplink and downlink transmission in two distinct time slots. For DSS, the whole Tx and Rx procedure requires double time related to the communication session within the coverage range. In Fig. 14, it is worth noticing that for DSS and SS, the portions of the spectrum used for Tx and Rx are different; for example,
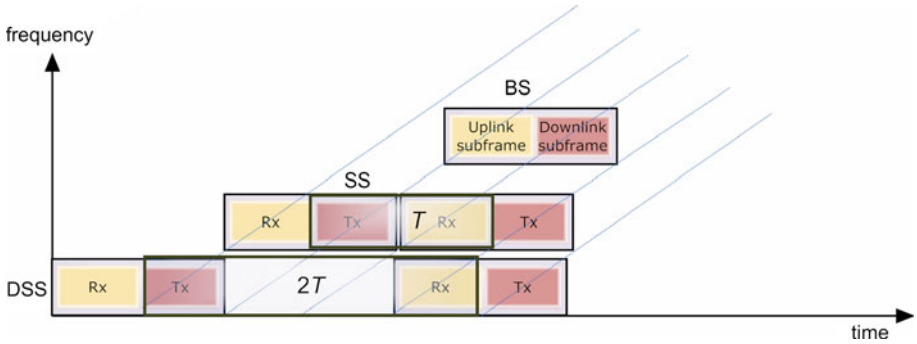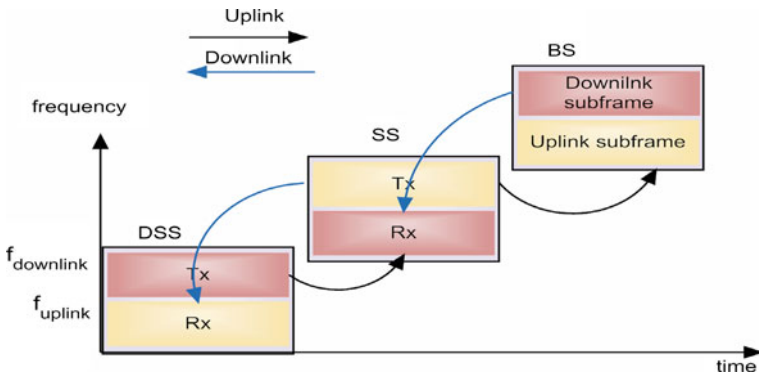
Fig. 13 DB for I-WiMAX in TDD scheme

Fig. 14 DB for I-WiMAX in FDD scheme

DSS must transmit signals to SS via adopting a spectrum band of the downlink. This is a hard task for such hardware modification. Therefore, TDD scheme is more flexible and more suitable for introducing DB into I-WiMAX.

There are two most relevant relay strategies: Amplify-and-forward (AF) and decode-and forward (DF) [60]. In the AF, the relay simply transmit the scaled and phase-shifted version of their received signals, while in the DF scheme, the relay starts with decoding and then re-encode their received signals prior to retransmitting them. We can see from Fig. 13 that in the TDD mode, since Tx and Rx are performed in different time slots, both AF and DF can be adopted. In this study, we consider the AF strategy because of its low complexity.

3.2 Multi-beam's Generating Method

The geometry structure of the relay network in our case is illustrated in Fig. 15. The kth node of the relay network is the kth SS, with the polar coordinates (r_k, Ψ_k). The location coordinates of the DSS are given by (A_i, ϕ_i), $i = 1, 2, \ldots, N_d$, where N_d is the number of DSS. For a total number of SS equal to N, we furthermore consider the following assumptions which are the same as in [18]. The location of each SS is chosen randomly, following a uniform distribution within a disk of radius R. Meanwhile, we assume that all SS transmit identical energies and that the path losses of all SS are also identical, meaning no multipath fading or shadowing. Next, no mutual coupling effects in the antenna of each SS are taken
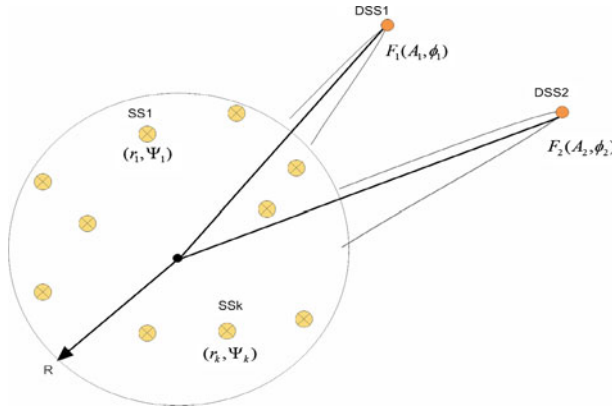
Fig. 15 Geometry structure of the relay network and DSS for DB

into account. We also assume that all the SS are perfectly synchronized so that no frequency offset or phase jitter exist.

If we chose the initial phase of each SS as

$$\Phi_k = -\frac{2\pi}{\lambda} d_k(A_1, \phi_1) \tag{18}$$

where

$$d_k(A_1, \phi_1) = \sqrt{A_1^2 + r_k^2 - 2A_1 r_k \cos(\Psi_k - \phi_1)} \approx A_1 - r_k \cos(\Psi_k - \phi_1) \tag{19}$$

denotes the far-field Euclidean distance between the kth SS and the 1st DSS. The far-field beampattern array factor for the set of SS is then approximated by

$$F(\phi \,|r_k, \Psi_k) \approx \frac{1}{N} \sum_{k=1}^{N} \exp\left\{ j\frac{2\pi}{\lambda} r_k[\cos(\phi_1 - \Psi_k) - \cos(\phi - \Psi_k)] \right\} \tag{20}$$

The locations of SS follow the uniform distribution over the disk of radius R. Thus, the probability density functions (pdf) are

$$f_{r_k}(r) = \frac{2r}{R^2}, \quad 0 \le r < R; \; f_{\Psi_k}(\Psi) = \frac{1}{2\pi}, \quad -\pi \le \Psi_k < \pi \tag{21}$$

By introducing $\tilde{r}_k \overset{\Delta}{=} r_k/R$, $\tilde{\Psi}_k \overset{\Delta}{=} \Psi_k - (\phi_1 + \phi)/2$, $z_k \overset{\Delta}{=} \tilde{r}_k \sin(\tilde{\Psi}_k)$, the compound random variable z_k has the following pdf, as shown in [18],

$$f_{z_k}(z) = \frac{2}{\pi}\sqrt{1 - z^2}, \quad -1 \le z < 1 \tag{22}$$

Then the array factor in Eq. (20) can be written as

$$F(\phi \,|z_k) = \frac{1}{N} \sum_{k=1}^{N} \exp\left[-j4\pi \tilde{R} \sin\left(\frac{\phi - \phi_1}{2}\right) z_k \right] \tag{23}$$

where $\widetilde{R} \triangleq R/\lambda$ is the radius of the disk normalized by the wavelength. The far field beam-pattern can be defined as

$$P(\phi \,|z_k\,) \triangleq |F(\phi \,|z_k\,)|^2 = \frac{1}{N} + \frac{1}{N^2} \sum_{k=1}^{N} \exp(-j\alpha(\phi)z_k) \sum_{l=1,l\neq k}^{N} \exp(j\alpha(\phi)z_l) \quad (24)$$

where $\alpha(\phi) = 4\pi \widetilde{R} \sin\left(\frac{\phi-\phi_1}{2}\right)$.

The average array beampattern of the random distributed SS becomes [18]

$$P_{av}(\phi) \triangleq \mathrm{E}_z[P(\phi \,|z_k\,)] = \frac{1}{N} + \left(1 - \frac{1}{N}\right)\mu^2(\phi) \quad (25)$$

where

$$\mu(\phi) = \left|\frac{2J_1(\alpha(\phi))}{\alpha(\phi)}\right| \quad (26)$$

and $J_n(\cdot)$ stands for the nth order Bessel function of the first kind.

If we adopt the initial phase as given in Eq. (18), it means that the average array pattern generated by the SS relay network towards (A_1, ϕ_1) can be expressed by Eq. (25). However, we can set an initial phase for SS different from Eq. (18), as for example has been shown in [18]. For adopting initial phases as given by Eq. (18), the synchronization of each SS requires an accurate knowledge on the distance, relative to the wavelength, between each node and the absolute distance. It is then possible to realize a closed-loop case as in self phasing arrays, and may be achieved by the use of reference signals such as comes from the Global Positioning System (GPS) [18].

The average beampattern in Eq. (25) does not show the probability for a certain amount of energy that may be received at different ϕ. This problem has still not yet been addressed. We therefore give now the CDF of $P(\phi \,|z_k\,)$, $Prob\{P(\phi \,|z_k\,) \,|P(\phi \,|z_k\,) \leq P_0\}$ when N is large. In Eq. (23), when N is large we know that according to the Central Limit Theorem, $F(\phi \,|z_k\,)$ satisfies the Gaussian distribution, i.e. $F(\phi \,|z_k\,) \sim \mathrm{N}(\mu(\phi), \frac{1-\mu^2(\phi)}{N})$. Then the absolute value of $F(\phi \,|z_k\,) - \mu(\phi)$ obeys the Rayleigh distribution. Finally, we obtain

$$Prob\{P(\phi \,|z_k\,) \,|P(\phi \,|z_k\,) > P_0\} = 1 - Prob\{P(\phi \,|z_k\,) \,|P(\phi \,|z_k\,) \leq P_0\}$$

$$= 1 - [F(|\mu(\phi)| + \sqrt{P_0}) - \frac{\mathrm{sgn}(|\mu(\phi)| - \sqrt{P_0}) + 1}{2} F(|\mu(\phi)| - \sqrt{P_0})] \quad (27)$$

where $F(x_0) = Prob(x \,|x \leq x_0\,) = 1 - \exp(-x_0^2 N/(1 - \mu^2(\phi)))$ for $x \geq 0$, is the CDF of the Rayleigh distribution of $P(\phi \,|z_k\,)$, and $\mathrm{sgn}(x) = |x| /x$.

The proof of equation (27) is shown in Appendix B.

Figure 16 shows the result of Eq. (27), indicating the probability distribution of the energy larger than P_0 with spreading over different ϕ. We here considered different $\widetilde{R}$ with $N = 256$, and $P_0 = 0.8$. We assumed only one DSS and a DOA of $\phi = 0$. From Fig. 16, we can see that with larger $\widetilde{R}$, at the same probability of more than 80% the energy focuses closer to the direction of DSS1.

Using Eqs. (18) and (25), it is easy to generate one beam towards one direction at the time: consequently the forming of more beams needs more time. Next, we present two methods to form more than one beam in space at the same time. Those beams belong to different DSS users when they receive signals within the same spectrum band.
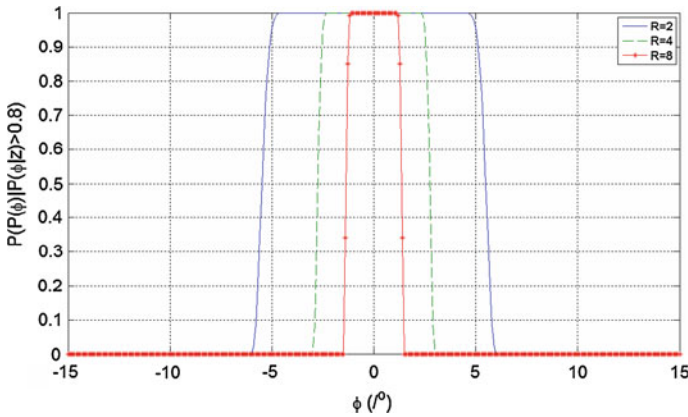
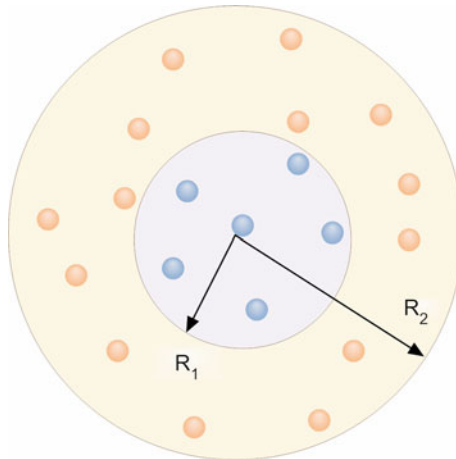**Fig. 16** The probability of $P(\phi\,|z_k) > 0.8$

Fig. 17 The proposed Multi-beam generating method of DB by separation of SS into a ring range and a circle range

3.2.1 Beampattern of Nodes Distributed in a Ring Range

We here discuss the case when nodes of networks are distributed in a ring range, rather than in a circle. Figure 17 shows the structure and parameters.

We assume that the locations of SS which are in the ring range follow the uniform distribution over the ring in the radius interval $R_2 - R_1$. Thus, the pdf's are

$$f_{r_k}(r) = \frac{2r}{R_2^2 - R_1^2}, \quad R_1 \le r_k < R_2; \quad f_{\Psi_k}(\Psi) = \frac{1}{2\pi}, \quad -\pi \le \Psi_k < \pi \tag{28}$$

Similarly, we can write for the average far-field beampattern of SS distributed in a ring range

$$P_{av}^{ring}(\phi) = \frac{1}{N} + \left(1 - \frac{1}{N}\right) \frac{[\mu(\phi) - \xi^2 v(\phi)]^2}{(1 - \xi^2)^2} \tag{29}$$

where $\xi = \frac{R_1}{R_2}$, $v(\phi) = \frac{2J_1(\xi\alpha(\phi))}{\xi\alpha(\phi)}$.

The proof of Eq. (29) is shown in Appendix C.

Then by separating SS into different groups, we synchronize them with different initial phases. For example, all SS located in the inner circle will have the initial phases of $\Phi_k^{\text{circle}} = -\frac{2\pi}{\lambda} d_k(A_1, \phi_1)$, while for those SS, which are in the ring range, we adopt different initial phases of $\Phi_k^{ring} = -\frac{2\pi}{\lambda} d_k(A_2, \phi_2)$. Then we have two beams towards both (A_1, ϕ_1) and (A_2, ϕ_2). If we need to direct beams towards more than two directions, we can separate SS, located in the outer circle of Fig. 17, into several different ring ranges with different radii.

3.2.2 DB with Nodes Having Randomly Selecting Phases

Another method to display more than one beam at the same time slot is to let the SS randomly chose which DSS to serve. If the kth SS chose the ith DSS to transmit signals, it will set the initial phases as $\Phi_k = -\frac{2\pi}{\lambda} d_k(A_i, \phi_i)$, $i = 1, 2, \ldots, N_d$. The chance that SS chose DSS is equal to $1/N_d$. In this case, the far-field beampattern of the SS relay network yields

$$F(\phi \,|\eta_k, r_k, \Psi_k) = \frac{1}{N} \sum_{k=1}^{N} \exp\left[-j4\pi \widetilde{R} \sin\left(\frac{\phi - \eta_k}{2}\right) \sin\left(\frac{2\Psi_k - \phi - \eta_k}{2}\right)\right] \quad (30)$$

where η is a discrete random variable, which has the following pdf

$$Prob(\eta \,|\eta = \phi_i) = \frac{1}{N_d}, \quad i = 1, 2, \ldots, N_d \quad (31)$$

Then the average array beampattern of the random distributed SS with random selected initial phased becomes

$$P_{av}(\phi) \triangleq \mathrm{E}_z[P(\phi \,|\eta_k, r_k, \Psi_k)]$$

$$= \sum_{i=1}^{N_d} \mathrm{E}_z[P(\phi \,|r_k, \Psi_k, \eta_k = \phi_i)] \cdot Prob(\eta \,|\eta = \phi_i)$$

$$= \frac{1}{N} + \frac{1}{N_d} \sum_{i=1}^{N_d} \left[\left(1 - \frac{1}{N}\right) \mu_i^2(\phi)\right] = \frac{1}{N} + \left(1 - \frac{1}{N}\right)\left[\frac{1}{N_d} \sum_{i=1}^{N_d} \mu_i(\phi)\right]^2 \quad (32)$$

where

$$\mu_i(\phi) = \frac{2J_1(\alpha_i(\phi))}{\alpha_i(\phi)}, \quad \alpha_i(\phi) = 4\pi \widetilde{R} \sin\left(\frac{\phi - \phi_i}{2}\right), \quad i = 1, 2, \ldots, N_d.$$

The results of the two multi-beam generating methods discussed above are shown in Fig. 18. We here consider the case $N = 256$, $\widetilde{R}_2 = 2$. For the first multi-beam generating method, $\xi = \frac{R_1}{R_2} = \frac{1}{3}$. We chose the SS in the inner circle to form a beam towards $\phi_1 = 0$, while the rest direct the beam at direction of $\phi_2 = 60°$. We can see that with both methods, two beams towards two required directions operate successfully. The beampattern of SS, distributed in a ring range, has higher sidelobes than that of a circle range. In the ring range case, the number of the SS is about $N\xi^2$, while that of the rest SS in a circle is $N(1 - \xi^2)$. According to [18], the sidelobe approaches $1/N$ as the beam angle moves away from the target direction, which explains the 8dB difference in sidelobe asymptote of the two beam patterns formed by SS in a circle and in a ring range. When the SS randomly chooses its initial phases, the beampattern tends to have two beams towards ϕ_1, ϕ_2 with half of the energy each. This is the result of an equally chance of selecting different initial phases.
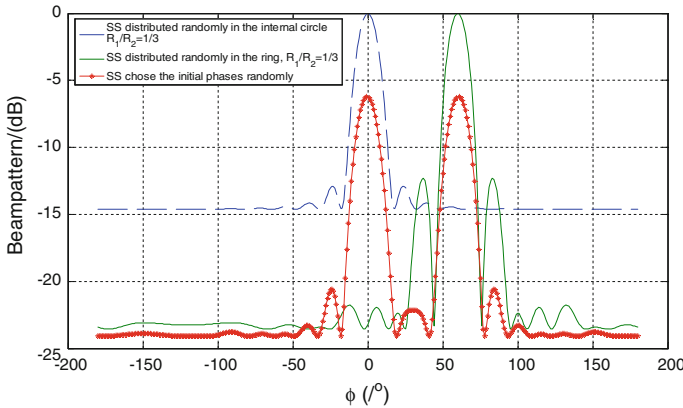
Fig. 18 DB with beampatterns of two multi-beam generating methods $\phi_1 = 0$, $\phi_2 = 60°$

Applying the DB method to the OFDM signal, different subcarriers are required to adopt different initial phases, because they operate at different frequency bands. The initial phases based on Eq. (18) for the ith subcarrier of the kth mode can be expressed as:

$$\Phi_{k,i} = -\frac{2\pi}{\lambda_i} d_k(A_1, \phi_1) = -\frac{2\pi}{c}(f_0 + (i-1)\Delta f)d_k(A_1, \phi_1), \quad i = 1, 2, \ldots, N_f \quad (33)$$

We assumed here N_f OFDM subcarriers, with frequency spacing Δf between two adjacent subcarriers, and f_0 is the starting frequency of the operating band.

From Eq. (25), the average beampattern of the ith subcarrier can be written as

$$P_{av,i}(\phi) \triangleq \mathrm{E}_z[P_i(\phi \,|z_k\,)] = \frac{1}{N} + (1 - \frac{1}{N})[\mu^{(i)}(\phi)]^2 \quad (34)$$

where

$$\mu^{(i)}(\phi) = \left| \frac{2J_1(\alpha^{(i)}(\phi))}{\alpha^{(i)}(\phi)} \right|,$$

$$\alpha^{(i)}(\phi) = 4\pi \widetilde{R_0}\left(1 + \frac{\Delta f(i-1)}{f_0}\right)\sin\left(\frac{\phi - \phi_i}{2}\right), \quad i = 1, 2, \ldots, N_d,$$

$$\widetilde{R_0} = \frac{R}{c}f_0$$

For WiMAX, there are three frequency bands defined in the standard, 2.5 and 3.5 GHz licensed spectrum, and the unlicensed 5 GHz spectrum [61]. The subcarrier spacing of Wi-MAX is always 10.94 kHz, which means when the available bandwidth increases, the number of subcarriers will also increases. WiMAX supports the channel bandwidth of 1.25, 5, 10, and 20 MHz. We assume that $f_0 = 3.5$ GHz, and the channel band is 1.25 MHz. Therefore, 128 subcarriers will be used. Then

$$\frac{\Delta f(i-1)}{f_0} \leq \frac{10.94 \times 127}{3.5} \times 10^{-6} \approx 4 \times 10^{-4} \ll 1, \quad i = 1, 2, \ldots, N_d, \quad (35)$$

Therefore,

$$\widetilde{R_0}\left(1 + \frac{\Delta f(i-1)}{f_0}\right) \approx \widetilde{R_0} \quad (36)$$

It means that in this case the average beampatterns of the all subcarriers are approximately the same.

Meanwhile, since the coverage of mobile WiMAX in an out door scenario is about 1 km, we can choose the radius R of the circle, where the SS are distributed, as large as 1 km to include more nodes in the relay network. Meanwhile we estimate $\widetilde{R_0} = \frac{R}{c} f_0 \gg 1$. It has been discussed in [18] that the 3-dB bandwidth of the average beampattern equals

$$\phi_{av}^{3dB} = 2 \arcsin\left(\frac{0.1268}{\widetilde{R_0}}\right) \tag{37}$$

As a result, in our case of WiMAX, the 3-dB bandwidth of the average main beam will be very small, in other words, the main beam is quite narrow. It is desirable to achieve a narrow main beam. However, when DSS is moving or the location of DSS is not accurate enough, too narrow beams may cause problems, as the DSS may not be covered by the main beam.

4 Conclusions

I-WiMAX, as a new maritime wireless communication system, promises a large coverage range, high data rates, efficient spectrum usage, and reliable communications in sea/lake scenarios. It consists of SR and mobile WiMAX. SR introduces two beamforming techniques, AB and DB, for ultimate efficient spectrum utilization and large coverage.

AB for uplink can spatially select the receiving signals of interested SS and alleviate co-channel interferences by directing the main beam towards the interested SS and nulls towards others. For downlink adaptive beamforming, the NB method is introduced in I-WiMAX to display spread nulls in a certain range of directions. We propose a new NB method, called VDA which is based on the MVDR beamformer. The VDA guarantees deeper nulls than CMT, while keeping the same width, and consequently decreasing co-channel interferences effectively and improving the coverage range significantly. What is more, the weights of different OFDM subcarriers with NB can be calculated iteratively, which reduces the computational complexity. When taking into account a spatial channel model, as is seen at the SS, it proves that NB is an essential part of I-WiMAX when serving reliable links to more than one SS within the same spectrum bands.

For SS (far) beyond the possible communication coverage range, we propose a relay network formed by those accessible SS to transmit the signals further to distant SS, rather than involving another BS. Due to the uncertainty of the location of the relay nodes, DB is employed for the SS relay network to transmit signals collaboratively after adopting different initial phases. We showed that the TDD mode of WiMAX is more suitable than FDD. However, sharing the spectrum requires directing more than one beam at the same time towards different DSS. Therefore, we proposed two methods of generating multiple beams. Both of them are able to focus transmitting energy on the requested directions. As a result, different DSS can receive signals from BS constructively with efficient spectrum utilization.

Appendix A

Proof of Equation (9)

From Eqs. (6) and (7), the element of the mth row and nth column of the covariance matrix can be written as

$$(\widetilde{\boldsymbol{R}}_{\mathrm{CMT},k})_{m,n} = (R_k)_{m,n}\mathrm{sinc}\left[\frac{(m-n)W}{2}\right] \tag{A-1}$$

Then by using the approximation proposed in Eq. (8), we can write

$$(\widetilde{\boldsymbol{R}}_{\mathrm{CMT},k})_{m,n} \approx (R_k)_{m,n}\left[1 - \frac{4}{3}\sin^2\left(\frac{\pi(m-n)W}{2\times 3}\right)\right]$$

$$= \frac{1}{3}(R_k)_{m,n} + \frac{2}{3}\sum_{i=0}^{N-1}\widehat{\sigma}_i^2 e^{j\frac{2\pi}{\lambda}x_m\sin\theta_i}\cos\left(\frac{\pi W}{3}\right)e^{-j\frac{2\pi}{\lambda}x_n\sin\theta_i}\cos\left(\frac{\pi W}{3}\right)$$

$$+ \frac{2}{3}\sum_{i=0}^{N-1}\widehat{\sigma}_i^2 e^{j\frac{2\pi}{\lambda}x_m\sin\theta_i}\sin\left(\frac{\pi W}{3}\right)e^{-j\frac{2\pi}{\lambda}x_n\sin\theta_i}\sin\left(\frac{\pi W}{3}\right)$$

$$\triangleq \widetilde{\boldsymbol{R}}_k \tag{A-2}$$

where x_m, x_n are the element locations of array antenna.

If we adopt the definitions of $\boldsymbol{D}_1, \boldsymbol{D}_2$ in Eqs. (10) and (11), $\widetilde{\boldsymbol{R}}_k$ can be easily written as $\widetilde{\boldsymbol{R}}_k = \frac{1}{3}\boldsymbol{R}_k + \frac{2}{3}\boldsymbol{D}_1\boldsymbol{R}_k\boldsymbol{D}_1 + \frac{2}{3}\boldsymbol{D}_2\boldsymbol{R}_k\boldsymbol{D}_2$, which is shown in Eq. (9).

Appendix B

Proof of Equation (27)

If we let

$$X \triangleq F(\phi\,|z_k)$$

$$Y \triangleq |F(\phi\,|z_k) - \mu(\phi)|$$

we then obtain

$$X \sim \mathrm{N}(\mu(\phi),\ \frac{1-\mu^2(\phi)}{N})$$

$$Y \sim \mathrm{Rayleigh}(\sigma_r^2)$$

According to the properties of the Rayleigh distribution,

$$E(y^2) = \sigma_r^2 2^{2/2}\Gamma\left(1+\frac{1}{2}\right) = 2\sigma_r^2 \tag{B-1}$$

On the other hand,

$$E(y^2) = \mathrm{E}[(x-\mu(\phi))^2] = \frac{1-\mu^2(\phi)}{N} \tag{B-2}$$

Then from Eqs. (B-1) and (B-2), we obtain

$$\sigma_r^2 = \frac{1-\mu^2(\phi)}{2N} \tag{B-3}$$

We calculate the probability $Prob\{P(\phi\,|z_k)\,|P(\phi\,|z_k) > P_0\}$, which is equal to

$$1 - Prob\{P(\phi\,|z_k)\,|P(\phi\,|z_k) \leq P_0\}.$$

We next discuss the outcome for the different cases.

If $|\mu(\phi)| > \sqrt{P_0}$, $y \in [|\mu(\phi)| - \sqrt{P_0},\ \ |\mu(\phi)| + \sqrt{P_0}]$,
then

$$Prob(x\,|x^2 \le P_0) = F(|\mu(\phi)| + \sqrt{P_0}) - F(|\mu(\phi)| - \sqrt{P_0}) \tag{B-4}$$

If $|\mu(\phi)| < \sqrt{P_0}$, $y \in [0, |\mu(\phi)| + \sqrt{P_0}]$,
then

$$Prob(x\,|x^2 \le P_0) = F(|\mu(\phi)| + \sqrt{P_0}) \tag{B-5}$$

where

$$F(y_0) = Prob(y\,|y \le y_0) = 1 - \exp\left(-y_0^2/2/\sigma_r^2\right)$$
$$= 1 - \exp(-y_0^2 N/(1 - \mu^2(\phi))) \tag{B-6}$$

To combine (B-4) and (B-5), it is easy to verify Eq. (27)

$$Prob\left\{x^2\,|x^2 > P_0\right\} = 1 - Prob\left\{x^2\,|x^2 \le P_0\right\}$$
$$= 1 - \left[F(|\mu(\phi)| + \sqrt{P_0}) - \frac{sgn(|\mu(\phi)| - \sqrt{P_0}) + 1}{2}\right.$$
$$\left. \times F(|\mu(\phi)| - \sqrt{P_0})\right]$$

Appendix C

Proof of Equation (29)

We define

$$u_k \overset{\Delta}{=} \frac{r_k}{R_2} \sin \frac{\phi + \phi_0 - 2\Psi_k}{2} \tag{C-1}$$

By adopting the method in [18], we can calculate the pdf of random variable u_k,

$$f_{U_k}(u_k) = \begin{cases} \frac{1}{\pi(1-\xi^2)}\sqrt{1 - u_k^2}, & \xi < u_k \le 1 \\[2mm] \frac{1}{\pi(1-\xi^2)}\left(\sqrt{1 - u_k^2} - \sqrt{\xi^2 - u_k^2}\right), & |u_k| \le |\xi| \\[2mm] \frac{1}{\pi(1-\xi^2)}\sqrt{1 - u_k^2}, & -1 \le u_k < -\xi \end{cases} \tag{C-2}$$

Then we can obtain the expectation of $\exp(-j\alpha(\phi)u_k)$ by

$$E[\exp(-j\alpha(\phi)u_k)]$$
$$= \frac{1}{\pi(1 - \xi^2)}\left[\int_{-1}^{1}\sqrt{1 - u_k^2}\exp(-j\alpha(\phi)u_k)du_k - \int_{-\xi}^{\xi}\sqrt{\xi^2 - u_k^2}\exp(-j\alpha(\phi)u_k)du_k\right]$$
$$= \frac{1}{1 - \xi^2}\left[\mu(\phi) - \xi^2\frac{2J_1(\alpha(\phi)\xi)}{(\alpha(\phi)\xi)}\right] = \frac{1}{1 - \xi^2}\left[\mu(\phi) - \xi^2 v(\phi)\right] \tag{C-3}$$

From Eqs. (24) and (25), we derive

$$
\begin{aligned}
P_{av}^{ring}(\phi) &= \mathrm{E}[P(\phi \,|z_k)] \\
&= \frac{1}{N} + \frac{1}{N^2}\mathrm{E}\left[\sum_{k=1}^{N}\exp(-j\alpha(\phi)u_k)\sum_{l=1,l\neq k}^{N}\exp(j\alpha(\phi)u_l)\right] \\
&= \frac{1}{N} + \frac{N-1}{N}[\mathrm{E}(\exp(-j\alpha(\phi)u_k))]^2 \\
&= \frac{1}{N} + \frac{N-1}{N}\frac{[\mu(\phi) - \xi^2 v(\phi)]^2}{(1-\xi^2)^2}
\end{aligned}
\tag{C-4}
$$

which shows the same results as in Eq. (29).

References

1. Lian, X., Nikookar, H., & Ligthart, L. (2010). Application of Green Radio to Maritime Coastal/Lake Communications and Locationing Introducing Intelligent WiMAX (I-WiMAX). In *Towards green ICT* (pp. 287–305). Aalborg: River Publisher.
2. Claudio, E. D., & Parisi, R. (2001). WAVES: Weighted average of signal subspaces for robust wideband direction finding. *IEEE Transactions on Signal Processing, 49*(10), 2179–2190.
3. Barrett, M., & Arnott, R. (1994). Adaptive antennas for mobile communications. *IEE Electronic & Communications Engineering Journal*, pp. 203–214.
4. Mizuno, M., & Takeo, O. (2007). Application of adaptive array antennas to radio communications. *Electronics and Communications in Japan, 77*(2), 48–59.
5. Tsoulos, G. V., Beach, M. A., & Swales, S. C. (1997). On the sensitivity of the capacity enhancement of a TDMA system with adaptive multibeam antennas. In *Proceedings of IEEE 47th VTC* (Vol. 1, pp. 165–169). Phoenix, USA, 4–7 May, 1997.
6. Nicoli, M., Sala, M., Simeone, O., Sampietro, L., & Santacesaria, C. (2007). Adaptive array processing for time-varying interference mitigation in IEEE802.16 systems. In *Proceedings of PIMRC* (pp. 1–5). Athens, Greece, 3–7 September, 2007.
7. Porter, J. W., Kepler, J. F., Krauss, T. P., Vook, F. W., Blankenship, T. K., Desai, V., et al. (2007). An experimental adaptive beamforming system for the IEEE802.16e-2005 OFDMA downlink. In *Proceedings of IEEE RWS* (pp. 475–478). Orlando, USA, 22–25 January, 2007.
8. Desai, V., Kepler, J. F., & Vook, W. (2007). Field data showing the downlink adaptive beamforming gains in an experimental IEEE802.16e-2005 OFDMA system. In *Proceedings of IEEE RWS* (pp. 619–622). Orlando, USA, 22–25 January, 2007.
9. Li, Y., & Kenyon, D. (2005). An examination of the processing complexity of an adaptive antenna system for WiMAX. In *Proceedings of the 2nd IEE/EURASIP conference on DSPenabledRadio* (pp. 7–13). Glasgow, UK, 19–20 September, 2005.
10. Ogawa, Y., & Ohgane, T. (1996). Adaptive antennas for future mobile radio. *IEICE Transaction Fundamentals, E79-A*(7), 961–967.
11. Swales, S. C., Beach, M. A., Edwards, D. J., & McGeehan, J. P. (1990). The performance enhancement of multibeam adaptive base-station antennas for cellular land mobile radio systems. *IEEE Transaction on Vehicle Technology, 39*(1), 56–67.
12. Aderson. N., & P. Howard. (1997). Technology and transceiver architecture considerations for adaptive antenna systems. In *Proceedings of ACTS Summit* (pp. 965–970), 1997.
13. Strandell, J., Wennstrom, M., Rydberg, A., Oberg, T., Gladh, O., Rexberg, L., et al. (1997). Experimental Evaluation of an adaptive antenna for TDMA mobile telephony system. In *Proceedings of PIMRC* (pp. 79–84). Helsinki, Finland, 1–4 September, 1997.
14. Monot, J. J., Thibault, J., Chevalier, P., Pipon, F., Mayrargue S., & Levy, A. (1997). A fully programmable prototype for the experimentation of the SDMA concept and use of smart antennas for

UMTS and GSM/DCS 1800 network. In *Proceedings of PIMRC* (pp. 534–538). Helsinki, Finland, 1–4 September, 1997.

15. Blogh, J. S., & Hanzo, L. (2002). *Third-generation systems and intelligent wireless networking smart antennas and adaptive modulation*. New York, NY: Wiley.

16. Hugl, K., Laurila, J., & Bonek, E. (1999). Downlink performance of adaptive antenna with null broadening. In *Proceedings of IEEE VTC* (pp. 872–876). Houston, USA, 4–7 May, 1999.

17. Lo, T. Y. (1972). A mathematical theory of antenna arrays with randomly spaces elements. *IEEE Transaction on Antennas and Propagation, 12*(3), 129–136.

18. Ochiai, H., Mitran, P., Poor, H. V., & Tarokh, V. (2005). Collaborative beamforming for distributed wireless ad hoc sensor networks. *IEEE Transaction on Signal Processing, 53*(11), 4110–4124.

19. Dong, L., Petropulu, A. P., & Poor, H. V. (2008). A cross-layer approach to collaborative beamforming for wireless ad hoc networks. *IEEE Transaction on Signal Processing, 56*(7), 2981–2993.

20. Zarifi, K., Affes, S., & Ghrayeb, A. (2009). Distributed beamforming for wireless sensor networks with random node location. In *Proceedings of ICASSP* (pp. 2261–2264). Taipei, Taiwan, 19–24 April, 2009.

21. Mudumbai, R., Barriac, G., & Madhow, U. (2007). On the feasibility of distributed beamforming in wireless sensor networks. *IEEE Transaction on Wireless Communication, 6*(5), 1754–1763.

22. Brown, D. R., III, & Poor, H. V. (2008). Time-slotted round-trip carrier synchronization for distributed beamforming. *IEEE Transaction on Signal Processing, 56*(11), 5630–5643.

23. Bucklew, J. A., & Sethares, W. A. (2008). Convergence of a class of decentralized beamforming algorithms. *IEEE Transaction on Signal Processing, 56*(6), 2280–2288.

24. Lian, X., Nikookar, H., & Ligthart, L. P. (2009). Adaptive OFDM beamformer with constrained weights for cognitive radio. In *Proceedings of IEEE VTC Spring* (pp. 1–5). Barcelona, Spain, 26–29 April, 2009.

25. Applebaum, S. P., & Chapman, D. J. (1976). Adaptive array with main beam constrains. *IEEE Transactions on Antennas and Propagation, 24*(5), 650–662.

26. Applebaum, S. P. (1976). Adaptive arrays. *IEEE Transactions on Antennas and Propagation, 24*(5), 585–598.

27. Widrow, B., Mantey, P. E., Griffiths, L. J., & Goode, B. B. (1967). Adaptive antenna systems. *Proceedings of IEEE, 55*(12), 2143–2159.

28. Frost, O. L. (1972). An algorithm for linearly constrained adaptive array processing. *Proceedings of IEEE, 60*(8), 926–935.

29. Griffiths, L. J. (1969). A simple adaptive algorithm for real-time processing in antenna arrays. *Proceedings of IEEE, 57*(10), 696–1704.

30. Gordara, L. C. (1969). Application of antenna arrays to mobile communications, Part II: Beam-forming and Direction-of-Arrival considerations. *Proceedings of IEEE, 85*(8), 1193–1245.

31. Capon, J. (1969). High-resolution frequency-wavenumber spectrum analysis. *Proceedings of IEEE, 57*(8), 1408–1418.

32. Reed, I. S., Mallett, J. D., & Brennan, L. E. (1974). Rapid convergence rate in adaptive arrays. *IEEE Transaction on Aerospace and Electronic Systems, 10*(6), 853–863.

33. Litva, J. (1996). *Digital beamforming in wireless communications*. Boston, London: Artech House.

34. Godara, L. C. (1997). Application of antenna arrays to mobile communications, Part I: performance improvement, feasibility, and system considerations. *Proceedings of IEEE, 85*(7), 1029–1060.

35. Krim, H., & Viberg, M. (1996). Two decades of array signal processing research. *IEEE Signal Processing Magazine*, pp. 67–94.

36. Treichler, J. R., & Agee, B. (1983). A new approach to multipath correction of constant modulus signals. *IEEE Transaction on Acoustics, Speech and Signal Processing, 31*(2), 459–472.

37. Godard, D. N. (1980). Self-recovering equalization and carrier tracking in a two-dimensional data communication system. *IEEE Transaction on Communication, 28*(11), 1867–1875.

38. Agee, B. G., Schell, S. V., & Gardner, W. A. (1990). Spectral self-coherent restoral: A new approach to build adaptive signal extraction using antenna arrays. *Proceedings of IEEE, 78*(4), 753–767.

39. Wu, Q., Wong, K. M., & Ho, R. (1994). A fast algorithm for adaptive beamforming of cyclic signals. *IEE Proceedings on Radar, Sonar and Navigation, 141*(6), 312–318.

40. Henriksson, J. A. (1987). Decision-directed diversity combiners-principles and Simulation results. *IEEE Journal on Selected Areas in Communications, 5*(3), 515–523.

41. Rappaport, T. S. (1996). *Wirelss communications: Principles and practice*. New Jersey: Prentice Hall.

42. Bell, K. L., Ephraim, Y., & Van Trees, H. L. (2000). A Bayesian approach to robust adaptive beamforming. *IEEE Transaction on Signal Processing, 48*(2), 386–398.

43. Lam, C. J., & Singer, A. C. (4445). Bayesian beamforming for DOA uncertainty: Theory and implementation. *IEEE Transaction on Signal Processing, 54*(11), 4435–4445.

44. Filho, D. Z., Panazio, C. M., Cavalcanti, F. R. P., & Romano, J. M. T. (2001). On downlink beamforming techniques for TDMA/FDD systems. In *Proceedings of Symposio Brasileiro de Telecomunicacoes*, Fortaleza, Brazil, 20 December, 2001.

45. Liang, Y. C., & Chin, F. P. S. (2002). FDD DS-CDMA Downlink beamforming by modifying uplink beamforming weights. In *Proceedings of IEEE VTC Fall* (pp. 170–174), Vancouver, Canada, 24–28 September, 2002.

46. Liang, Y. C., Chin, F. P. S., & Liu, K. J. R. (2001). Downlink beamforming for DS-CDMA mobile radio with multimedia services. *IEEE Transaction on Communication, 49*(7), 1288–1298.

47. Mailloux, R. J. (1998). Covariance matrix augmentation to produce adaptive array pattern troughs. *Electronics Letters, 31*(10), 771–772.

48. Zatman, M. (1998). Production of adaptive array troughs by dispersion synthesis. *Electronics Letters, 31*(25), 2141–2142.

49. Guerci, J. R. (1999). Theory and application of covariance matrix tapers for robust adaptive beamforming. *IEEE Transaction on Signal Processing, 47*(4), 977–985.

50. Song, H. C., Kuperman, W. A., Hodgkiss, W.S., Gerstoft, P., & Kim, J. S. (2004). Robustness of null broadening against source motion. In *Proceedings of Sensor Array and Multichannel Signal Processing Workshop* (pp. 470–474), Washington, USA, 4–6 August, 2004.

51. Song, H. C., Kuperman, W. A., Hodgkiss, W. S., Gerstoft, P., & Kim, J. S. (2003). Null broadening with snapshot-deficient covariance matrices in passive sonar. *IEEE Journal of Oceanic Engineering, 28*(2), 250–261.

52. Riba, J., Goldberg, J., & Vazquez, G. (1997). Robust beamforming for interference rejection in mobile communications. *IEEE Transaction on Acoustic Speech, Signal Processing, 45*(1), 271–275.

53. Hugl, K., Laurila, J., & Bonek, E. (1999). Downlink performance of adaptive antennas with null broadening. In *Proceedings of IEEE 49th VTC* (pp. 16–20), Houston, USA, 16–20 May, 1999.

54. Xu, Z., & Zakharov, Y. (2007). Modified null broadening adaptive beamforming: Constrained optimization approach. *Electronics Letters, 43*(3), 145–146.

55. Yang, Y., & Wan, C. (2004). Adaptive beampattern synthesis based on broadening. In *Proceedings of IEEE Antennas and Propagation Society International Symposium* (pp. 3996–3999), California, USA, 20–25 June, 2004.

56. Adali, T., & Haykin, S. (2010). *Adaptive signal processing: Next generation solutions*. New Jersey: Wiley.

57. Stuber, G. L. (1996). *Principles of mobile communication*. Boston, MA: Kluwer.

58. Sadowsky, J. S., & Kafedziski, V. (1998). On the correlation and scattering functions of the WSSUS channel for mobile communication. *IEEE Transaction on Vehicle Technology, 47*(1), 270–282.

59. Abdi, A., Barger, J. A., & Kaveh, M. (2002). A parametric model for the distribution of the angle of arrival and the associated correlation function and power spectrum at the mobile station. *IEEE Transaction on Vehicle Technology, 51*(3), 425–434.

60. Laneman, J. N., Tse, D. N. C., & Wornell, G. W. (2004). Cooperative diversity in wireless networks: Efficient protocols and outage behavior. *IEEE Transaction on Information Theory, 50*(12), 3062–3080.

61. Johnston, N., & Aghvami, H. (2007). Comparing WiMAX and HSPA—A guide to the technology. *BT Technology Journal, 25*(2), 191–199.

Author Biographies

Xiaohua Lian received her B.S. and M.S. degrees in electrical and electronic engineering from Nanjing University of Aeronautics and Astronautics (NUAA), Nanjing, China, in 2002 and 2005, respectively. She is now working towards her Ph.D. in Delft University of Technology in the Nederlands. Her research interests include array signal processing for radar and for wireless communications, smart antenna and cognitive radio, etc.

Homayoun Nikookar received his Ph.D. in Electrical Engineering from Delft University of Technology (TUDelft), The Netherlands, in 1995. From 1995 to 1998 he was a post doctoral research fellow at the International Research Centre for Telecommunications and Radar (IRCTR) of the Faculty of Electrical Engineering, Mathematics and Computer Science (EEMCS) of TUDelft, and since 1999 serves as a faculty member of the Telecommunications Department of EEMCS of TUDelft where he is currently an Associate Professor. Dr. Nikookar is also the leader of the Radio Advanced Technologies and Systems (RATS) program of IRCTR, leading a team of researchers carrying out cutting-edge research in the field of wireless radio transmission. He has conducted active research in many areas of wireless communications, including wireless channel modeling, Ultra Wideband, MIMO, multicarrier transmission, Wavelet-based OFDM and Cognitive Radio. He has published over 100 papers, in refereed international conferences and journals. He is also the recipient of several paper awards of IEEE journals and International Conferences and Symposiums. In 2007 Dr. Nikookar served as the Chair of the 14th IEEE Symposium on Communications and Vehicular Technology (SCVT) in Benelux and in 2008 was the Chairman of the European Wireless Technology Conference (EuWiT) in Amsterdam. He has been technical program committee member of several international conferences and has served as a Guest Editor of several international journals. He is a senior member of the IEEE and the coauthor of the book, *Introduction to Ultra Wideband for Wireless Communications*, Springer, 2009.

Leo P. Ligthart was born in Rotterdam, the Netherlands, on September 15, 1946. He received an Engineer's degree (cum laude) and a Doctor of Technology degree from Delft University of Technology in 1969 and 1985, respectively. He is fellow of IEE and IEEE. He received Doctorates (honoris causa) at Moscow State Technical University of Civil Aviation in 1999, Tomsk State University of Control Systems and Radioelectronics in 2001 and Military Technical Academy, Romania in 2010. He is academician of the Russian Academy of Transport. Since 1992, he has held the chair of Microwave Transmission, Radar and Remote Sensing in the Faculty of Electrical Engineering, Mathematics and Computer Science, Delft University of Technology. In 1994, he founded the International Research Center for Telecommunications and Radar (IRCTR) and has been the director of IRCTR for more than 16 year. His principal areas of specialization include antennas and propagation, radar and remote sensing, but he has also been active in satellite, mobile and radio communications. He has published over 600 papers and book chapters, and 2 books.